Tetraphenylethylene-Based Multicomponent Emissive Metallacages as Solid-State Fluorescent Materials

*Chaoqun Mu, Zeyuan Zhang, Yali Hou, Haifei Liu, Lingzhi Ma, Xiaopeng Li, Sanliang Ling, Gang He, Mingming Zhang**

Abstract: *The construction of solid-state fluorescent materials with high quantum yield and good processability is of vital importance in the preparation of organic light-emitting devices. Herein, a series of tetraphenylethylene-based multicomponent emissive metallacages are prepared by the coordination-driven self-assembly of tetra-(4-pyridylphenyl)ethylene, cis-Pt(PEt$_3$)$_2$(OTf)$_2$ and tetracarboxylic ligands. These metallacages exhibit good emission both in solution and in the solid state because the coordination bonds and aggregation restrict the molecular motions of TPE synergistically, which suppresses the non-radiative decay of these metallacages. Impressively, one of the metallacages achieves very high fluorescence quantum yield (Φ_F = 88.46%) in the solid state, which is further used as the coatings of a blue LED bulb to achieve white-light emission. The study not only provides a general method to the preparation of TPE-based metallacages but also explores their applications as solid-state fluorescent materials, which will promote the future design and applications of metallacages as useful emissive devices.*

Light-emitting materials have attracted increasing interest owing to their widespread applications as chemical sensors,[1] organic light-emitting diodes (OLEDs)[2] and contrast agents for cell imaging,[3] etc. Compared with inorganic luminescent materials, organic ones not only possess good solution processability but also are cost-effective and easy to fabricate, making them good candidates for flexible displays. However, most conventional organic fluorophores tend to aggregate, causing their emission to be quenched in concentrated or in the solid state (aggregation-caused quenching, ACQ).[4] In order to solve this problem, Tang et al. developed a type of fluorophores that is nearly non-emissive in dilute solution while emits strongly in the aggregated state, which is termed as aggregation-induced emission (AIE).[4,5] As star molecules in this field, tetraphenylethylene (TPE) and its derivatives[6] are the most widely studied fluorophores due to their ease of preparation and functionalization. These molecules have been widely used for the preparation of OLEDs with good fluorescence quantum yields (Φ_F) in the solid state.[6]

Metal-coordination interactions have proved to be a powerful tool to the construction of metal organic frameworks (MOFs) [7] and supramolecular coordination complexes (SCCs).[8] It has been found that the incorporation of TPE derivatives into MOFs and SCCs gives a series of emissive MOFs[9] and SCCs[10] because the metal-coordination bonds restrict the molecular motions of the aromatic groups on TPE, reducing the non-radiative decay in the excited state and thus giving bright emission (also known as coordination-induced emission, CIE). Emissive MOFs[9] are generally used as bulk crystalline materials because their poor solubility in common solvents constrain their processability. Emissive SCCs[10] provide an alternative candidate especially for the applications in solution, but most of them are non-emissive in the solid state. The combination of good processability and high solubility and solid-state emission in a single supramolecular entity has been rarely addressed. The exploration of emissive metallacages with good emission in the solid state and atomistic insights on the aggregation mode will offer a type of processable and tunable organic light-emitting materials. Therefore, such metallacages are urgently needed to be developed.

Herein, through the integration of AIE and CIE (Scheme 1), a type of TPE-based multicomponent emissive metallacages (MEMs) that show excellent solid-state emission is developed. These MEMs are prepared by the metal-coordination-driven self-assembly of tetra-(4-pyridylphenyl)ethylene (**1**), tetracarboxylic ligands (**2a**–**2d**) and *cis*-Pt(PEt$_3$)$_2$(OTf)$_2$ (**3**) (Scheme 2). This multicomponent system not only offers more abundant structures compared with two-component system, but also gives a pathway to finely tune the structures and the emission properties of a given fluorescent pyridyl ligand just by changing carboxylic ligands during the self-assembly. These MEMs show moderate emission in acetonitrile solution and their AIE properties are well retained. Moreover, they emit strongly in the solid state, with Φ_F reaches as high as 88.46% for metallacage **4a**, which is among the highest values for metallacages in the solid state.[10a-10h] It can be concluded from the crystal structure that the coordination and aggregation restrict the molecular motions synergistically (Scheme 1), offering very high Φ_F for the metallacages. Owing to the good solubility of metallacage **4a,** it can be easily coated on the surface a blue LED bulb. Because of its yellow emission color, white LEDs (WLEDs) are obtained based on phosphor conversion. This study combines AIE and CIE to achieve highly emissive materials in the solid state, which will promote the use of emissive SCCs as light-emitting devices.

[*] C. Mu, Dr. Z. Zhang, Y. Hou, H. Liu, L. Ma, Prof. M. Zhang
State Key Laboratory for Mechanical Behavior of Materials, Shaanxi International Research Center for Soft Matter, School of Materials Science and Engineering, Xi'an Jiaotong University, Xi'an 710049, P. R. China
E-mail: mingming.zhang@xjtu.edu.cn
L. Ma, Prof. X. Li
College of Chemistry and Environmental Engineering, Shenzhen University, Shenzhen 518055, P. R. China
Dr. S. Ling
Advanced Materials Research Group, Faculty of Engineering, University of Nottingham, Nottingham, NG7 2RD, United Kingdom
Prof. G. He
Frontier Institute of Science and Technology, Xi'an Jiaotong University, Xi'an 710049, P. R. China

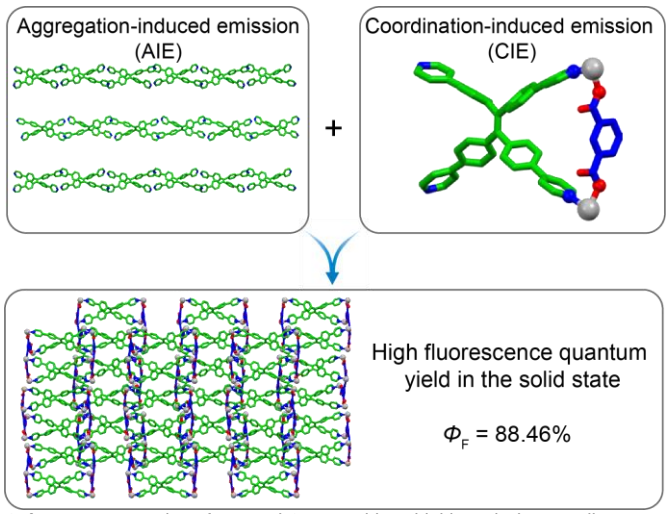

Scheme 1. Integration of AIE and CIE to achieve highly emissive metallacages in the solid state.

The formation of MEMs **4a**–**4d** were supported by $^{31}P\{^1H\}$, ^1H NMR and electrospray ionization time-of-flight mass spectrometry (ESI-TOF-MS) (Figure 1). The $^{31}P\{^1H\}$ spectra of MEMs **4a**–**4d** exhibited two doublets of equal intensity with concomitant ^{195}Pt satellites at 5.73 and 0.21 ppm for **4a**, 5.62 ppm and 0.17 ppm for **4b**, 5.42 ppm and 0.10 ppm for **4c** and 5.50 ppm and 0.09 ppm for **4d**, (Figure 1a–d), indicating the formation of discrete, charge-separated metallacages. In the ^1H NMR spectra (Figure 1e–i), downfield chemical shifts were observed for α-pyridyl protons H_a and β-pyridyl protons H_b of MEMs **4a**–**4d** owing to the coordination of the pyridyl moieties with the platinum atoms. The stoichiometries of MEMs **4a**–**4d** were evidenced by ESI-TOF-MS (Figure 1j-m). Dominated sets of peaks with charge states (from 3+ to 6+) were observed for all of the MEMs owing to the loss of counterions (OTf^-) and each peak agreed well with their simulated patterns. For example, peaks at m/z = 1175.8761, 1176.6697, 1196.6987 and 1236.8956 were found, corresponding to [**4a** – 5OTf]$^{5+}$, [**4b** – 5OTf]$^{5+}$, [**4c** – 5OTf]$^{5+}$ and [**4d** – 5OTf]$^{5+}$, respectively.

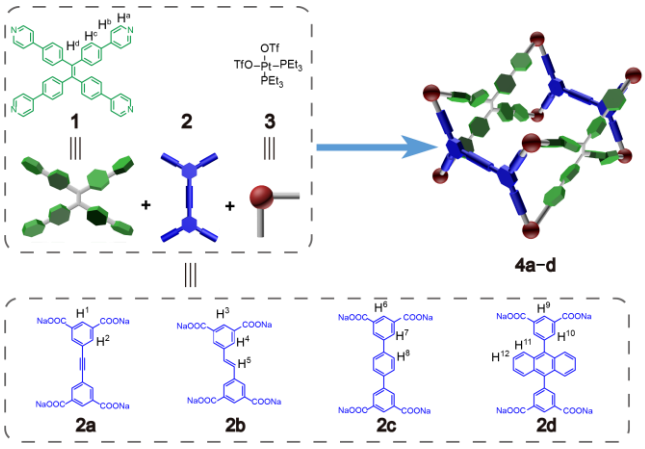

Scheme 2. Self-assembly of metallacages **4a**–**4d.**

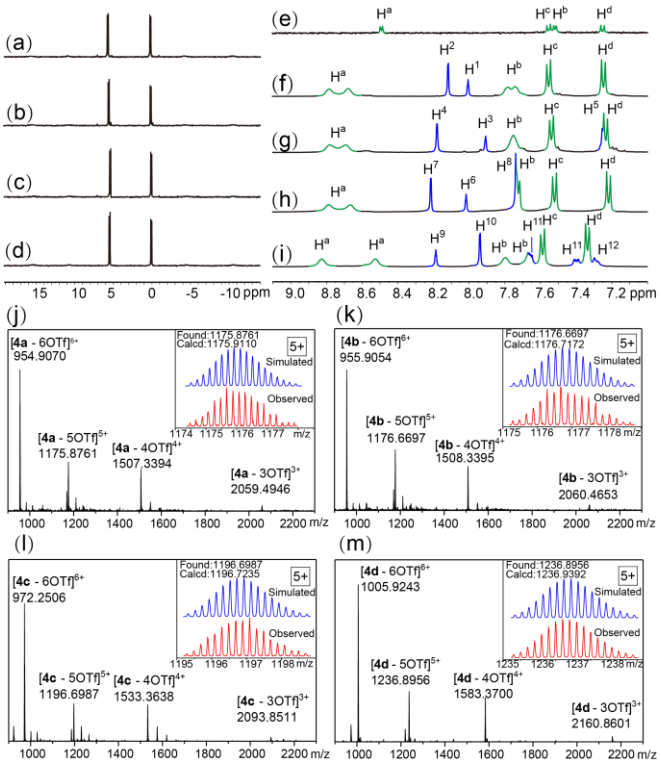

Figure 1. Partial $^{31}P\{^1H\}$ NMR (a–d) and ^1H NMR (e–i) spectra (162 or 400 MHz, CD_3CN, 295 K) **1** (e), **4a** (a, e), **4b** (b, f), **4c** (c, g) and **4d** (d, h). ESI-TOF-MS spectra of **4a** (j), **4b** (k), **4c** (l) and **4d** (m).

Single crystals of metallacage **4a** and **4d** suitable for X-ray diffraction analysis were grown by slow diffusion of dioxane into dimethyl formamide solution of **4a** for one month, and by slow diffusion of isopropyl ether into acetonitrile solution of **4d** for three weeks at 8°C, respectively. The solid-state crystal structure of **4a** and **4d** (Figure 2a–d) unambiguously confirmed their three-dimensional structures. To the best of our knowledge, these are the first TPE-based MEMs of which the crystal structures are resolved.[10a-10e] The crystal structures indicate that two TPE units and two carboxylic ligands are connected parallelly by eight Pt atoms, forming barrel-shaped metallacages with large windows. The length, width and height of **4a** and **4d** are 1.91 × 1.08 × 1.04 nm and 1.91 × 1.08 × 1.05 nm, respectively, based on the distance between Pt atoms. There is no perfect face-to-face arrangement between neighboring metallacages in the crystals (Figure S15). The relatively weak interactions between neighboring metallacages results in a crystal packing which is more disordered in the short range. Each unit cell of the MEM **4a** and **4d** crystals contains four and two metallacages, respectively, while a similar perylene diimide-based metallacage crystal contains only one metallacage in each unit cell.[10m] Although the metallacage possesses a three-dimensional cavity, no good host-guest chemistry was found for polycyclic aromatic hydrocarbons such as anthracene and thianthrene (Figure S16). It can be seen from the crystal structure that all the aromatic rings on TPE units are perpendicular to the two TPE faces, which makes it difficult for the guest molecules to form strong π-π stacking interactions with the faces, so the guest molecules are difficult to be encapsulated into the cavity. This is confirmed by density functional theory calculations (Figure S17), which show that both anthracene and thianthrene molecules prefer to locate between two neighboring metallacages than inside the cavity of a single metallacage, with the binding inside the cavity to be energetically less favorable by 16~21 kJ/mol.

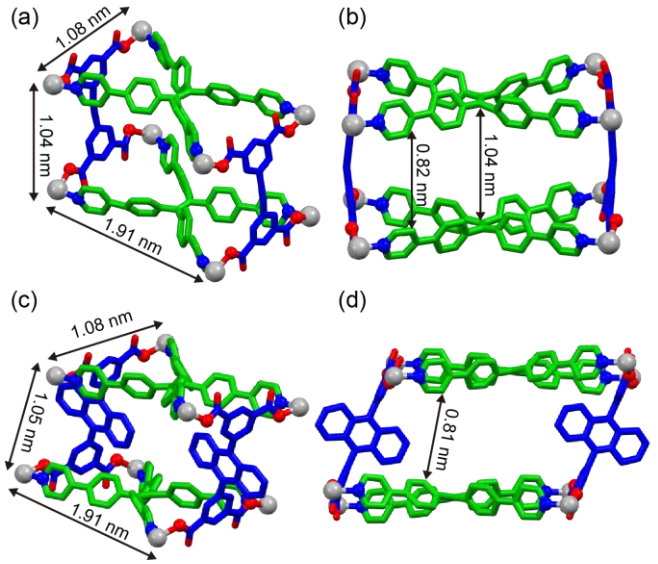

Figure 2. Crystal structure of **4a** (CCDC: 2055368) in different views: (a) front view and (b) side view. Crystal structure of **4d** (CCDC: 2068948) in different views: (c) front view and (d) side view. Hydrogen atoms, counterions, solvent molecules and triethylphosphine units are omitted for clarity.

Ligand **1** exhibits two absorption bands centered at 274 and 308 nm with molar absorption coefficients (ε) of 3.73×10^4 and 2.87×10^4 M^{-1} cm^{-1}, respectively (Figure 3a). Owing to the weak absorption of tetracarboxylic ligands **2a**–**c**, MEMs **4a**–**4c** also display two absorption bands centered at 266 and 286 nm for **4a**, 264 and 284 nm for **4b**, and 280 and 326 nm for **4c**, with $\varepsilon = 7.50 \times 10^4$ and 7.58×10^4 M^{-1} cm^{-1} (**4a**), 8.88×10^4 and 8.34×10^4 M^{-1} cm^{-1} (**4b**) and 1.26×10^5 M^{-1} and 8.10×10^4 cm^{-1} (**4c**). Due to the absorption of anthracene-based tetracarboxylic ligand **2d**, MEM **4d** shows a broad absorption band at 260 nm and a distinct shoulder at 368 nm with $\varepsilon = 1.34 \times 10^5$ and 6.53×10^4 $M^{-1}cm^{-1}$, respectively. Ligand **1** shows weak emission at 441 nm in acetonitrile (Figure 3b). However, the emissions of MEMs **4a**–**4d** are dramatically enhanced because the molecular motions of ligand **1** are restricted by coordination bonds, decreasing the non-radiative decay and thus giving bright emission. For MEMs **4a-c**, the maximum emissions exhibited bathochromic shifts to 515~518 nm with Φ_F = 29.48%, 48.27%, and 21.21%, respectively. This is because the metal-coordination bonds planarize the TPE units, decreasing the energy band gap and thus inducing the bathochromic shifts. MEM **4d** displays two emission peaks at 422 nm and 515 nm with Φ_F = 6.82%, corresponding to the typical emission bands of anthracene and TPE derivatives, respectively. The AIE effects of these MEMs were investigated by measuring the fluorescence spectra of increasing amount of water in acetonitrile (Figure 3c-f). The emissions of these MEMs decreased dramatically after the addition of 10% of water because the enhanced intramolecular charge transfer (ICT) process in polar solvents.[11] When the water fractions were over 60%, the emission of the system increased dramatically, which is a typical AIE effect. MEM **4d** also experienced a change of emission color from blue to green-yellow as the increase of water fractions. This is because anthracene derivatives are a type of ACQ fluorophores while TPE groups are typical AIE fluorophores and the enhanced energy transfer from ligand **2d** to ligand **1** in aggregate state (Figure S39)[5a,12]. At low water fractions (<50%), little aggregation happens and the ACQ fluorophores dominates the emission, so the solutions emit in blue. However, at high water fractions (>60%), the metallacages tend to aggregate and the AIE fluorophores play a leading role in fluorescence, so the emission color of the solutions is green-yellow. Based on the incorporation of fluorophores with different emission properties (AIE and ACQ), the emission color of a single SCC can be finely tuned simply by the changes of solvent compositions.

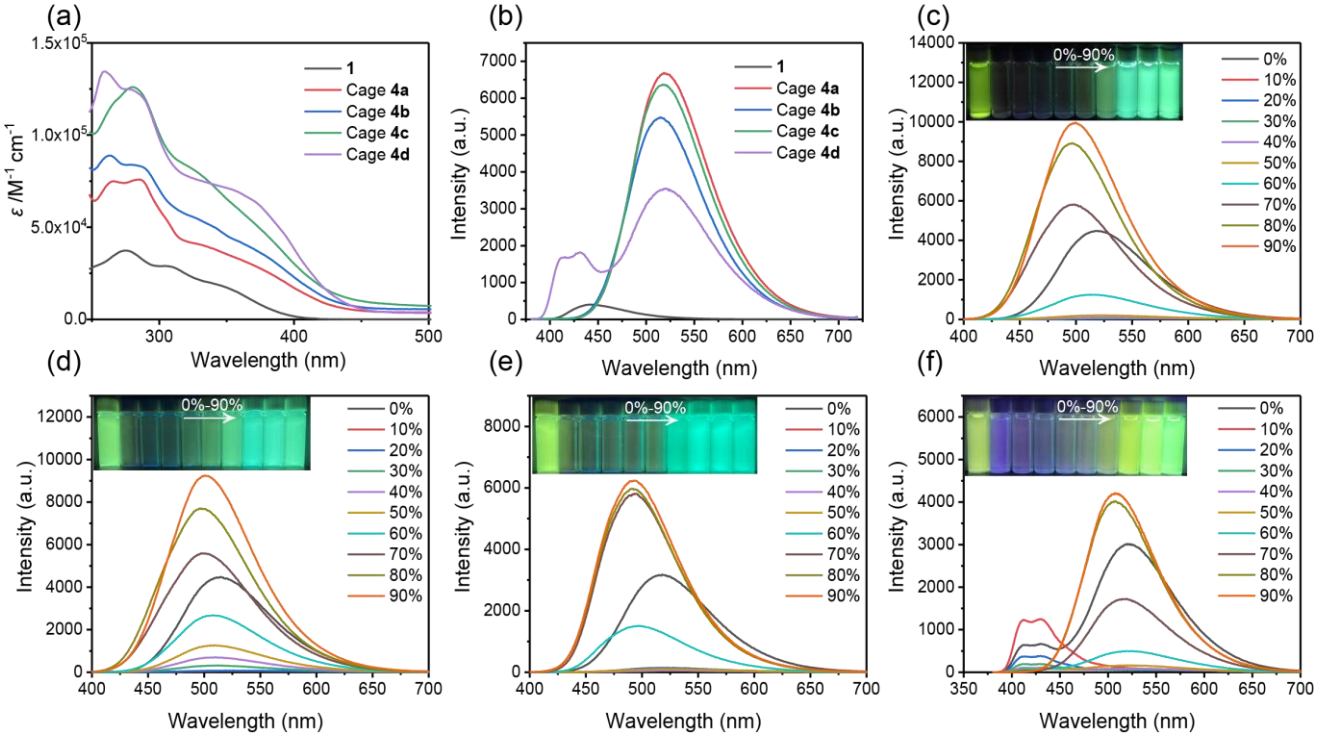

Figure 3. (a) UV/vis absorption and (b) fluorescence spectra of ligand **1** and metallacages **4a**−**4d** in acetonitrile. Fluorescence spectra of (c) **4a**, (d) **4b**, (e) **4c**, and (f) **4d** with different volume fractions of water in acetonitrile. Insets: photographs of **4a-d** in different fractions of water in acetonitrile upon excitation using an UV lamp at 298 K (λ_{ex} = 365 nm, c = 10.0 μM).

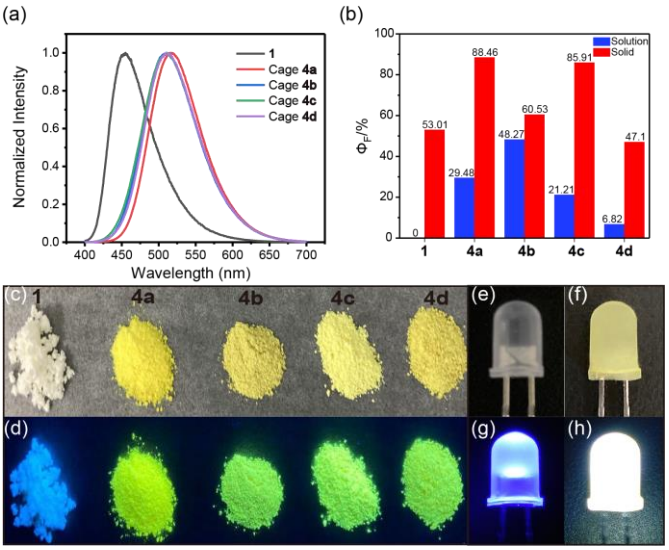

Figure 4. (a) Normalized fluorescence spectra of ligand **1** and metallacages **4a**–**4d** in the solid state. (b) Absolute fluorescence quantum yields of ligand **1** and metallacages **4a-4d** in acetonitrile and in the solid state. (c) Optical and (d) fluorescence photographs of the solid powders of ligand **1** and metallacages **4a**–**4d**. Photographs of (e, g) uncoated LED bulb, (f, h) coated LED bulb (e, f) before and (g, h) after illumination.

The normalized emissions of ligand **1** and MEMs **4a**–**4d** in the solid state were further studied. Ligand **1** exhibited an emission band centered at 454 nm (Figure 4a) with Φ_F = 53.01%, displaying a typical AIE effect. After the formation of metallacages, their maximum emission experienced a bathochromic shift to 510~517 nm, similar as that happened in solution. It is worth noting that the Φ_F values of MEMs **4a**–**d** are 88.46%, 60.53%, 85.91% and 47.1%, respectively (Figure 4b), which are among the highest values for metallacages in the solid state (Figure S27).[10a-10h] Although the emission of MEM **4d** is less than that of **1** because of the ACQ properties of the anthracene units in **4d**, the Φ_F of MEMs **4a**–**c** are all greater than that of **1**. This suggests that the solid emission of SCCs can be enhanced by aggregation and coordination synergistically. The emission color of MEMs **4a**–**d** is in the green-yellow region (Figure 4c and d), which is complementary with blue color. Considering the very high quantum yield of **4a** and its good solution processability, it was coated on a blue LED bulb to prepare WLEDs (Figure 4e–h) based on phosphor conversion. The blue LED bulb was simply dipped into the acetonitrile solution of **4a** for several times and then a thin and uniform film was formed on the surface of the bulb. Bright white light could be generated when a 3 V bias was applied. Two emission bands centered at 455 nm and 533 nm were found from the emission spectra (Figure S37), which covered the whole visible region to give white-light emission. According to the 1931 Commission Internationale deL'Eclairage chromaticity diagram, the coordinate is (0.28, 0.32), locating at the white-light zone.

In summary, TPE-based MEMs were constructed by the linkage of tetrapyridyl TPE and tetracarboxylic ligands using *cis*-$Pt(PEt_3)_2(OTf)_2$. Because both the aggregation and coordination could restrict the molecular motions of the aryl groups on TPE, these metallacages are emissive in solution and their fluorescence quantum yields increased dramatically in the solid state. Noticeably, due to the appropriate emission color, high fluorescence quantum yield and good solution processability, one of the MEMs was utilized as coatings for blue LED bulb to prepare WLEDs. This work not only provides a general strategy to the construction of TPE-based metallacages, but also explores their applications as the coating for WLEDs, which will promote the applications of emissive metallacages as solid-state fluorescent materials.

Acknowledgements

This work was supported by the National Natural Science Foundation of China (21801203) and The Key Research and Development Program of Shaanxi Province (2019KW-019). We thank Dr. Gang Chang and Yu Wang at Instrument Analysis Center and Dr. Aqun Zheng and Junjie Zhang at Experimental Chemistry Center of Xi'an Jiaotong University for NMR and fluorescence measurements. We are grateful for access to the University of Nottingham's Augusta HPC service.

Conflict of interest

The authors declare no conflict of interest.

Received: ((will be filled in by the editorial staff))
Published online on ((will be filled in by the editorial staff))

Keywords: aggregation-induced emission · coordination-induced emission · multicomponent emissive metallacages · solid-state fluorescent materials · self-assembly

[1] a) S. Shanmugaraju, P. S. Mukherjee, *Chem. Commun.* **2015**, *51*, 16014–16032; b) T. L. Mako, J. M. Racicot, M. Levine, *Chem. Rev.* **2019**, *119*, 322–477.

[2] a) M. P. Duffy, W. Delaunay, P.-A. Bouit, M. Hissler, *Chem. Soc. Rev.* **2016**, *45*, 5296–5310; b) V. W. Yam, V. K. Au, S. Y. Leung, *Chem. Rev.* **2015**, *115*, 7589–7728.

[3] a) S. Samanta, Y. He, A. Sharma, J. Kim, W. Pan, Z. Yang, J. Li, W. Yan, L. Liu, J. Qu; J. S. Kim, *Chem* **2019**, *5*, 1697–1726; b) L. Wang, M. S. Frei, A. Salim, K. Johnsson, *J. Am. Chem. Soc.* **2019**, *141*, 2770–2781.

[4] Y. Hong, J. W. Y. Lam, B. Z. Tang, *Chem. Soc. Rev.* **2011,** *40*, 5361–5388.

[5] a) J. Mei, N. L. Leung, R. T. Kwok, J. W. Lam, B. Z. Tang, *Chem. Rev.* **2015**, *115*, 11718–11940; b) Z. Zhao, H. Zhang, J. W. Y. Lam, B. Z. Tang, *Angew. Chem. Int. Ed.* **2020**, *59*, 9888–9907.

[6] a) Z. Zhao, J. W. Y. Lam, B. Z. Tang, *J. Mater. Chem.* **2012**, *22*, 23726–23740; b) J.-Y. Zhu, C.-X. Li, P.-Z. Chen, Z. Ma, B. Zou, L.-Y. Niu, G. Cui, Q.-Z. Yang, *Mater. Chem. Front.* **2020**, *4*, 176-181

[7] H. Furukawa, K. E. Cordova, M. O'Keeffe, O. M. Yaghi, *Science* **2013**, *341*, 1230444.

[8] a) Y. Inokuma, M. Kawano, M. Fujita, *Nat. Chem.* **2011**, *3*, 349–358; b) C. J. Brown, F. D. Toste, R. G. Bergman, K. N. Raymond, *Chem. Rev.***2015**, *115*, 3012–3035; c) T. R. Cook, P. J. Stang, *Chem. Rev.* **2015**, *115*, 7001–7045; d) W. Wang, Y. X.Wang, H. B. Yang, *Chem. Soc. Rev.* **2016**, *45*, 2656–2693; e) G. H. Clever, P. Punt, *Acc. Chem. Res.* **2017**, *50*, 2233–2243; f) S. Chakraborty, G. R. Newkome, *Chem. Soc. Rev.* **2018**, *47*, 3991–4016; g) F. J. Rizzuto, L. K. S. von Krbek, J. R. Nitschke, *Nat. Rev. Chem.* **2019**, *3*, 204–222; h) M. Yoshizawa, L. Catti, *Acc. Chem. Res.* **2019**, *52*, 2392–2404; i) Y. Sun, C. Chen, J. Liu, P. J. Stang, *Chem. Soc. Rev.* **2020**, *49*, 3889–3919; j) S. Tashiro, M. Shionoya, *Acc. Chem. Res.* **2020**, *53*, 632–643.

[9] a) N. B. Shustova, B. D. McCarthy, M. Dinca, *J. Am. Chem. Soc.* **2011**, *133*, 20126–20129; b) Q. Gong, Z. Hu, B. J. Deibert, T. J. Emge, S. J. Teat, D. Banerjee, B. Mussman, N. D. Rudd, J. Li, *J. Am. Chem. Soc.* **2014,** *136*, 16724–16727; c) M. Zhang, G. Feng, Z. Song, Y. P. Zhou, H. Y. Chao, D. Yuan, T. T. Tan, Z. Guo, Z. Hu, B. Z. Tang, B. Liu, D. Zhao, *J. Am. Chem. Soc.* **2014**, *136*, 7241–7244; d) Z.Wei, Z.-Y. Gu, R. K. Arvapally, Y.-P. Chen, R. N., Jr. McDougald, J. F. Ivy, A. A. Yakovenko, D. Feng, M. A. Omary, H.-C. Zhou, *J. Am. Chem. Soc.* **2014**, *136*, 8269–8276; e) X. Guo, N. Zhu, S. P. Wang, G. Li, F. Q. Bai, Y. Li, Y. Han, B. Zou, X. B. Chen, Z. Shi, *Angew. Chem. Int. Ed.* **2020,** *59*, 19716–19721; f) W. Shang, X. Zhu, T. Liang, C. Du, L. Hu, T. Li, M. Liu, *Angew. Chem. Int. Ed.* **2020**, *59*, 12811–12816.

[10] a) X. Yan, T. R. Cook, P. Wang, F. Huang, P. J. Stang, *Nat. Chem.* **2015,** *7*, 342–348; b) M. Zhang, M. L. Saha, M. Wang, Z. Zhou, B. Song, C. Lu, X. Yan, X. Li, F. Huang, S. Yin, P. J. Stang, *J. Am. Chem. Soc.* **2017**, *139*, 5067–5074; c) C. Lu, M. Zhang, D. Tang, X. Yan, Z. Zhang, Z. Zhou, B. Song, H. Wang, X. Li, S. Yin, H. Sepehrpour, P. J. Stang, *J. Am. Chem. Soc.* **2018**, *140*, 7674–7680; d) Z. Zhang, Z. Zhao, Y. Hou, H. Wang, X. Li, G. He, M. Zhang, *Angew. Chem. Int. Ed.* **2019**, *58*, 8862–8866; e) Z. Zhang, Z. Zhao, L. Wu, S. Lu, S. Ling, G. Li, L. Xu, L. Ma, Y. Hou, X. Wang, X. Li, G. He, K.

Wang, B. Zou, M. Zhang, *J. Am. Chem. Soc*. **2020,** *142*, 2592–2600; f) Y. Li, Y. An, J. Fan, X. Liu, X. Li, F. E. Hahn, Y. Wang, Y. Han, *Angew. Chem. Int. Ed*. **2020**, *59*, 10073–10080; g) J. Dong, Y. Pan, H. Wang, K. Yang, L. Liu, Z. Qiao, Y. D. Yuan, S. B. Peh, J. Zhang, L. Shi, H. Liang, Y. Han, X. Li, J. Jiang, B. Liu, D. Zhao, *Angew. Chem. Int. Ed.* **2020**, *59*, 10151–10159; h) G. Li, Z. Zhou, C. Yuan, Z. Guo, Y. Liu, D. Zhao, K. Liu, J. Zhao, H. Tan, X. Yan, *Angew. Chem. Int. Ed*. **2020,** *59*, 10013–10017; i) G. Q. Yin, H. Wang, X. Q. Wang, B. Song, L. J. Chen, L. Wang, X. Q. Hao, H. B. Yang, X. Li, *Nat. Commun.* **2018**, *9*, 567; j) L. J. Chen, Y. Y. Ren, N. W. Wu, B. Sun, J. Q. Ma, L. Zhang, H. Tan, M. Liu, X. Li, H. B. Yang, *J. Am. Chem. Soc*. **2015**, *137*, 11725–11735; k) P. Das, A. Kumar, P. Howlader, P. S. Mukherjee, *Chem. Eur. J.* **2017**, *23*, 12565–12574; l) T. Zhang, G. L. Zhang, Q. Q. Yan, L. P. Zhou, L. X. Cai, X. Q. Guo, Q. F. Sun, *Inorg. Chem.* **2018**, *57*, 3596–3601; m) Y. Hou,; Z. Zhang, S.Lu, J. Yuan, Q. Zhu, W. P. Chen, S. Ling, X. Li, Y. Z. Zheng, K. Zhu, M. Zhang, *J. Am. Chem. Soc.* **2020**, *142*, 18763–18768; n) X. Yan, P. Wei, Y. Liu, M. Wang, C. Chen, J. Zhao, G. Li, M. L. Saha, Z. Zhou, Z. An, X. Li, P. J. Stang, *J. Am. Chem. Soc*. **2019**, *141*, 9673–9679; o) C. Lu, M. Zhang, D. Tang, X. Yan, Z. Zhang, Z. Zhou, B. Song, H. Wang, X. Li, S. Yin, H. Sepehrpour, P. J. Stang, *J. Am. Chem. Soc*. **2018**, *140*, 7674–7680; p) A. Kumar, P. S. Mukherjee, *Chem. Eur. J*. **2020**, *26*, 4842–4849.

[11] a) G.-F. Zhang, M. P. Aldred, W.-L. Gong, C. Li, M.-Q. Zhu, *Chem. Commun.* **2012**, *48*, 7711–7713; b) R. Hu, E. Lager, A. Aguilar-Aguilar, J. Liu, J. W. Y. Lam, H. H. Y. Sung, I. D. Williams, Y. Zhong, K. S. Wong, E. Peña-Cabrera, B. Z. Tang, *J. Mater. Chem. C* **2009**, 113, 15845–15853.

[12] H.-Q. Peng, L.-Y. Niu, Y.-Z. Chen, L.-Z. Wu, C.-H. Tung, Q.-Z. Yang, *Chem. Rev*. **2015**, *115*, 7502–7542.

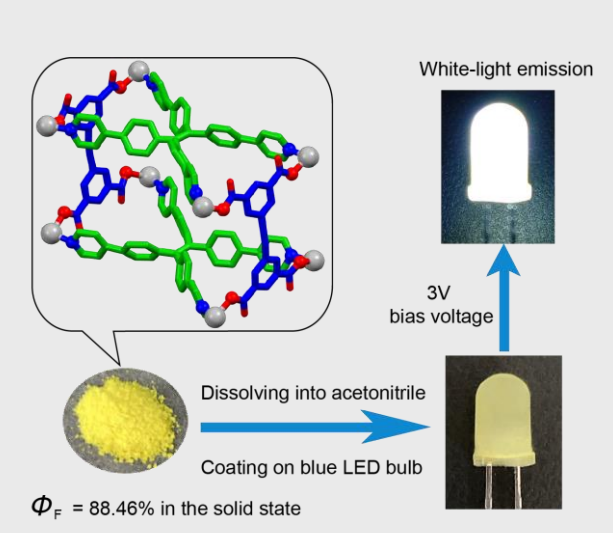

*Chaoqun Mu, Zeyuan Zhang, Yali Hou, Haifei Liu, Lingzhi Ma, Xiaopeng Li, Sanliang Ling, Gang He, Mingming Zhang**

Page No. – Page No.
Tetraphenylethylene-Based Multicomponent Emissive Metallacages as Solid-State Fluorescent Materials

Tetraphenylethylene-based multicomponent emissive metallacages with high fluorescence quantum yield and good processability were prepared. These metallacages were further utilized as coatings for blue light-emitting bulb to prepare white-light emitting diodes, demostrating their applications as solid-state fluorescent materials.